Proceedings of the
44th IEEE Conference on Decision and Control, and
the European Control Conference 2005
Seville, Spain, December 12-15, 2005

Controlled Hydrodynamic Interactions in Schooling Aquatic Locomotion

Scott D. Kelly and Hailong Xiong

Abstract— **We present experimental data elucidating the effects of hydrodynamic coupling on the propulsive efficiency of an array of three oscillating hydrofoils. We simulate this system using an inviscid flow model; this model duplicates certain key features of our experimental data but fails to consider the effects of wake vortex generation and interaction. We present a qualitative model for the role played by wake vortex dynamics in the cooperative locomotion of fish schools, and derive a mathematical model in the form of a nonlinear control system describing the interaction of a single deformable body with a single nearby vortex. We present simulations based on the latter to illustrate the capture of vortices shed from one fish in a school by a second, trailing fish; vortex capture in this sense is the control problem central to cooperative swimming.**

I. INTRODUCTION

Hydrodynamic coupling among fish swimming in a school can dramatically reduce the average drag experienced by individual fish in the school, and can thus improve the propulsive efficiency of the school as a whole. This fact has been documented in the biology literature [1], [2], [3], [4], [5], but the mechanism of coupling has been questioned, and its significance doubted, by some authors [6]. Existing models for the relevant hydrodynamics are rare and very simplified [7], [8], despite a growing literature on other dynamical aspects of fish schooling [9], [10], [11], [12]. This owes much to the unsteady nature of the fluid-solid interactions defining schooling locomotion. Drag reduction on bird flocks through tip-vortex cancellation — a phenomenon which has been modeled successfully and exploited by aircraft in formation — can, in contrast, be treated as a problem in steady flow [13].

Hydrodynamic schooling is a problem of engineering interest as well as scientific interest. Numerous efforts are ongoing within the robotics community to realize fishlike aquatic vehicles [14], [15], [16], [17], [18], [19], [20], motivated by the superiority of such designs in energy efficiency, maneuverability, and stealth [21], [22]. Schools of such vehicles promise, for example, a platform for reconfigurable mobile sensing applications ranging from environmental sampling to the collection of military intelligence [23]. Although energy efficiency is a primary concern in the design of mobile sensor arrays for long-term deployment, efforts to develop aquatic vehicle arrays for cooperative sensing [24], [25] have, to date, ignored the hydrodynamic coupling among vehicles as a means to conserve energy.

Support for this work was provided by NSF award number CMS-0449319
Department of Mechanical and Industrial Engineering, University of Illinois at Urbana-Champaign, Urbana, IL 61801, USA
scott.and.xiong@diffeomorphism.com

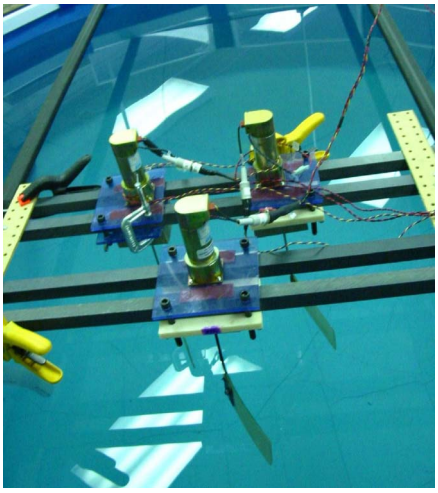

Fig. 1. Experimental hydrofoil array

II. HYDRODYNAMIC INTERACTIONS IN A SIMPLE HYDROFOIL ARRAY

The effects of hydrodynamic coupling on schooling locomotion are straightforward to reproduce in the lab; indeed, our experimental system allows us to detail these effects to an extent infeasible through observations of fish schools. Consider the robotic system shown in Figure 1. Three stiff rubber strips, each six inches long and four inches high, are submerged on vertical shafts in two rows to a depth of eight inches in a pool of water eight feet across. The three units are constrained to translate as a group across the pool as they oscillate, thrice per second each, propelling a support platform on wheels atop two rails. The independent motors which drive the oscillations can be seen mounted above the platform. The system can be configured so that two units lead one, or so that one unit leads two, across the pool.

The data we present corresponds to the configuration depicted in Figure 2 for this hydrofoil array. One foil leads two in the x direction and the foils are driven such that

$$\phi_1 = \sin \omega t, \quad \phi_2 = \sin(\omega t + \beta), \quad \phi_3 = \sin(\omega t + \alpha) \quad (1)$$

with $\omega \approx 18$ rad/s. We denote the longitudinal spacing between the lead foil and the trailing row by a and the lateral spacing in the trailing row by b.

Figure 3 depicts the displacement of the array as a function of time, with $\alpha = \beta = 0$, for two different interfoil spacings. The array's displacement after nine seconds with $a = 8$ inches and $b = 20$ inches is more than thrice that with $a = 7$ inches and $b = 6$ inches, suggesting that near-field

0-7803-9568-9/05/$20.00 ©2005 IEEE

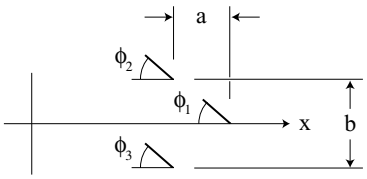

Fig. 2. Idealized hydrofoil array

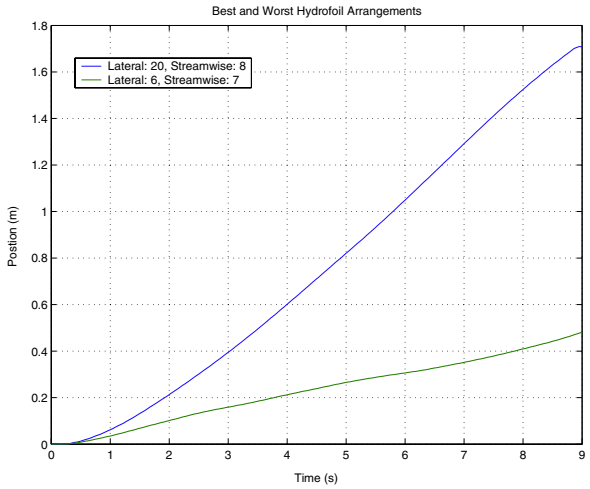

Fig. 3. Best-case and worst-case foil spacing with identical phasing

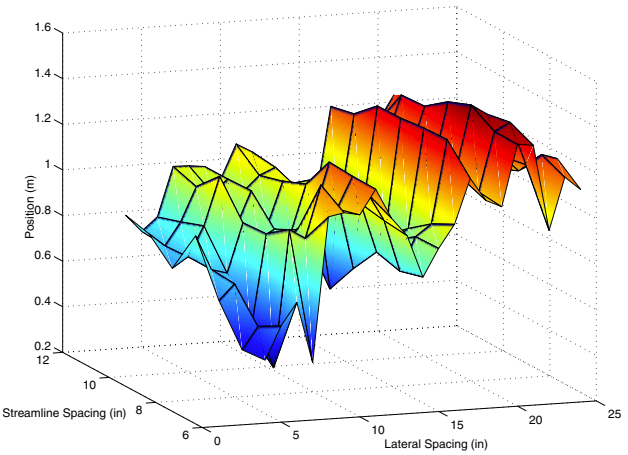

Fig. 4. Measured position after a fixed time as a function of foil spacing

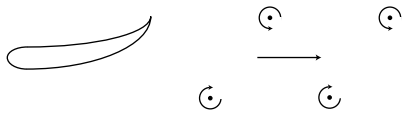

Fig. 5. A propulsive wake comprising discrete vortices

wake interactions among the foils are a severe impediment to propulsion in the latter case.

Figure 4, depicting the array's final displacement for several parametric combinations (a, b), however, reveals more detailed a dependence of efficiency on spacing. We note, in particular, that the final displacement oscillates as the lateral spacing b is increased.

A good photograph of the wake shed by a translating, oscillating hydrofoil — an inverse Kármán vortex street in the midplane of the foil — appears in [20]. Fish resembling members of family Carangidae — particularly fast and efficient swimmers [21], [22], and the inspiration for the majority of current fishlike robots — shed similar wakes. Such a wake is depicted in Fig. 5. The vortices shed at the extremes in the motion of the caudal fin of the fish are polarized such that fluid directly behind the fish is propelled to the right; the fish is propelled, correspondingly, to the left.

We believe interactions among the wakes shed by the three foils comprising our array, each wake approximating an inverse Kármán vortex street like that shown in Fig. 5, to mediate the efficiency of the array overall. In particular, we believe that when oppositely-polarized vortices shed by adjacent fish are superposed to cancel one another, the efficiency of the array is locally maximized. Our reasoning is detailed in Section IV; for now, we note that this model predicts periodicity like that in Fig. 4 with respect to both a and b when α and β are held fixed and with respect to both α and β when a and b are held fixed.

Periodicity in final distance with variations in a is difficult to discern in Fig. 4, in part, because our system comprises the smallest number of hydrofoils that might reasonably be called an array. Undamped periodicity would require an infinite array of foils. Periodicity with respect to both α and β with a and b held fixed is apparent, however, in Fig. 6. Individual data points represent integer pairs (m, n) parametrizing the gait (1) with

$$\alpha = \frac{m\pi}{6}, \qquad \beta = \frac{n\pi}{6}.$$

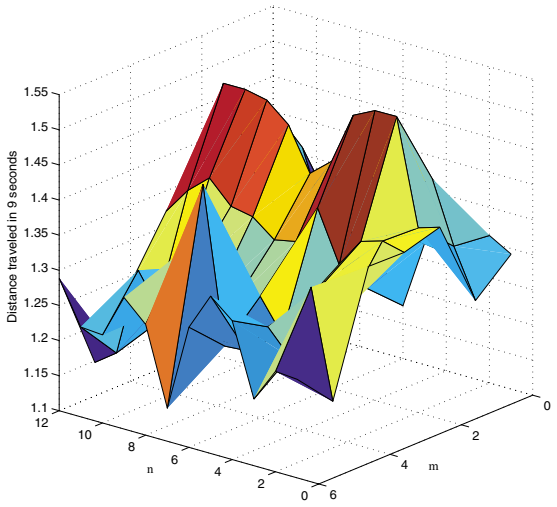

Fig. 6. Measured position after a fixed time as a function of foil phasing

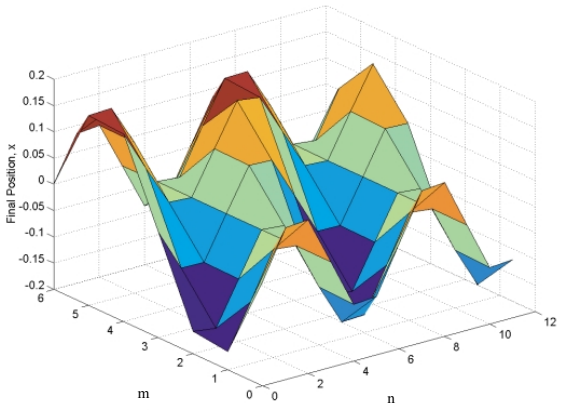

Fig. 7. Simulated position after a fixed time as a function of foil phasing

III. INVISCID HYDRODYNAMIC COUPLING

Although the flow through our experimental hydrofoil array is distinguished by periodic vortex structures, the fluid velocity field contains a component which is irrotational. An objective of the authors' is the comprehensive treatment of schooling locomotion as a problem in geometric mechanics, but the viscous phenomenon of vortex shedding exceeds the present scope of geometric methods. Hydrodynamic interactions among solid bodies in an irrotational flow field lend themselves readily to analytical methods like Lagrangian and Hamiltonian reduction, and irrotational models have recently been advanced for interacting systems of bodies immersed in fluids [26]. It is therefore worth exploring the validity of an irrotational model for our experimental system.

Figure 7 reproduces Figure 6 via numerical simulation assuming irrotational flow around the system shown in Fig. 2. It is noteworthy that the oscillatory dependence of final displacement on both α and β is apparent in Figure 7 despite the absence of vortex structures in the simulated flow. The mean final displacement of the array as a function of α and β, however, is predicted in Fig. 7 to be zero.

It is demonstrated in [27] that the self-propulsion of a deformable body — or of a system of bodies — in an irrotational flow can be described by a geometric construction called a *principal connection*. Consistent with Fig. 7, a mechanical system governed by a principal connection cannot derive net displacement from oscillatory deformations which enclose no area in the abstract space of variables parametrizing its shape. It is furthermore the case that models in the form of principal connections are invariant with respect to time scaling. Although we present experimental data for only one oscillatory frequency ω, the value of this frequency clearly influences the overall performance of our laboratory array. In the limit as ω approaches zero, in particular, it is clear that the laboratory array will not translate at all. We conclude that an accurate model for the self-propulsion of the real array must account for the dynamics of the array's vortical wake.

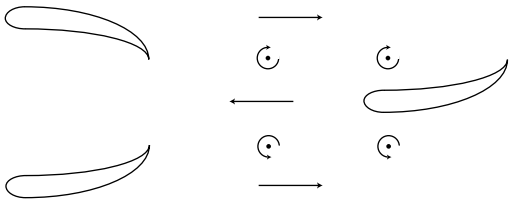

Fig. 8. One fish drafts the combined wake of two others

Fig. 9. Wake energy harvesting through vortex cancellation

We conclude this Section with a comparison of our experimental results to the predictions of the inviscid model presented in [8]. Our inviscid model represents the potential flow around three solid bodies in the absence of vortices; the model in [8] represents the potential flow through a translating, semi-infinite array of regularly-spaced vortices in the absence of solid bodies. The vortex array is assumed to be generated by a semi-infinite array of fish with oscillating caudal fins, but the fish are assumed to be hydrodynamically invisible, carried along by the flow between the vortices without interrupting it.

The latter model predicts that fish far from the front line in a semi-infinite array can experience, for the same fin motions, a five-fold increase in propulsive force through their interaction. This advantage would be diminished in an array of finite size; this is consistent with the three-and-a-half-fold range of swimming velocities shown in Figure 3. The analysis in [8] predicts, furthermore, that the most energy-efficient arrangement of fish in a school is constructed of units like that shown in Figure 2 with the longitudinal distance between consecutive rows roughly twice the lateral distance between consecutive fish in a given row. If, in particular, $a = 8$ inches, then fish in a given row should be separated by distances b which are multiples of 4 inches. The array configuration providing our best experimental results corresponds to $a = 8$ inches and $b = 20$ inches.

IV. VORTEX WAKE GENERATION AND WAKE-BODY INTERACTIONS

Our conceptual model for wake-body interactions in schooling locomotion is illustrated in Fig. 5 and in Figs. 8 through 10. We note, first of all, that energy imparted to the fluid by the fish in Fig. 5 is effectively lost to the wake.

A fish situated between the vortex streets trailing two other fish experiences an ambient flow assisting forward propulsion, as shown in Fig. 8. This is the basis for the schooling model presented in [8]. Energy can be further harvested by one fish in a school from the wake of another by counter-spinning a vortex trailing the latter at one extreme of the motion of the former's caudal fin, as shown in Fig. 9. The wake trailing the harvesting fish contains less lost energy than would that of a lone fish. Properly-timed oscillations in the shape of a fish's body — and thus in the

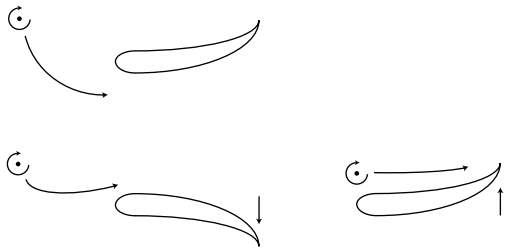

Fig. 10. Body oscillations direct incoming vortices

direction of the circulatory flow around its body — entrain incoming vortices for energy harvesting at the proper position relative to the caudal fin, as shown in Fig. 10. The fish which does not undulate loses the opportunity to exploit the incoming vortex when the vortex follows the circulatory flow counterclockwise around the fish.

In Section V we construct an explicit model for the motion of a single vortex in the presence of a hydrofoil undergoing prescribed deformations over time. This model allows us, in particular, to verify the need for control of the kind illustrated in Fig. 10, and to explore the proper timing of body undulations to provide for the energy extraction of Figure 9. The motion of the vortex is the result of four superposed flows, to wit

- The flow generated by the vortex itself. Although an isolated vortex will remain stationary in an unbounded fluid, the presence of the hydrofoil deforms the flow due to the vortex — introducing a self-advection term — in a manner that depends on the hydrofoil's instantaneous shape.
- The flow due to the deformation of the hydrofoil. The flow on the surface of the foil must have zero normal velocity relative to the foil, but fluid is permitted to slip along the foil.
- A uniform freestream flow relative to the hydrofoil. This is equivalent to the assumption that the foil is translating relative to quiescent fluid infinitely far away.
- A circulatory flow around the hydrofoil, varying in strength as the foil changes shape to enforce a Kutta condition at the foil's trailing point relative to the freestream flow. The addition of circulation to the inviscid flow over a rigid foil to prescribe the position of a trailing stagnation point is the basis for inviscid airfoil theory [28]. The treatment of Kutta conditions as constraints on fluid-body systems in the context of Lagrangian mechanics is introduced by the authors in [29].

It is noteworthy that we have chosen to account for circulatory flow around the hydrofoil but not for the shedding of new vorticity from the foil's trailing point to balance changes in this flow over time. In so doing, we have simplified our model considerably. We justify this simplification, in part, by noting that vorticity shed behind the foil will be carried downstream by the superposed uniform flow and will thus have minimal effect on the motion of the upstream vortex. A computational model which accounts for continuous vortex shedding in the formation of wake structures behind a translating, deforming foil appears in [30].

It is also noteworthy that our model addresses the motion of a free vortex subject to a *constant* freestream flow relative to a deforming foil. Although this is equivalent to the problem in which the foil itself translates, it is unlikely that the translation of a fish in a school is actually steady. The interactions of a free deforming body and a nearby vortex require a more complicated model. The authors and collaborators are working to develop Hamiltonian descriptions for extensions to the classical *Föppl problem* of a free rigid body interacting with a collection of vortices [31], [32], building upon their work in [33] and upon parallel work like that in [34].

V. DYNAMIC MODEL FOR WAKE VORTEX ENTRAINMENT

The treatment of ideal flow in the plane can often be simplified by associating a single complex coordinate with each point in the plane and specifying patterns of flow in terms of *complex potentials*. The complex potential $w(z)$ generates the velocity field in the complex z plane such that $\dot{z} = (dw/dz)^*$, where the symbol * indicates the complex conjugate of its argument.

It was noted in Section III that a flow model which excludes vortex dynamics will be inadequate to describe the phenomena underpinning schooling locomotion. Potential flow theory, however, accommodates both the treatment of discrete moving vortices and the treatment of circulatory flows around closed solid boundaries; we refer the reader to [35] for details. The modeling assumptions detailed in Section IV permit us to apply potential flow methods to the problem of a single deforming hydrofoil interacting with a free vortex.

The family of profiles realized in the complex ζ plane as images of circles in the complex z plane under the *Joukowski transformation*

$$\zeta = f(z) = z + \frac{k^2}{z}, \tag{2}$$

where k is a real constant, have received special attention in the literature of inviscid airfoil theory. We parametrize the deforming foil in our control problem as the image under this transformation of a circle with center $d = x_c + jy_c$ and radius R in the z plane, and we treat $\dot{x}_c$, $\dot{y}_c$, and $\dot{R}$ as control inputs.

It is clear that (2) will map any two points z and k^2/z to the same point in the ζ plane; the inverse transformation is given by

$$z = f^{-1}(\zeta) = \frac{1}{2}\left(\zeta \pm \sqrt{\zeta^2 - 4k^2}\right). \tag{3}$$

We restrict ourselves to the case $k < R$ and choose the positive square root when invoking the inverse map (3) to ensure that f^{-1} maps points outside the foil in the ζ plane to points outside the circle in the z plane.

A vortex with strength Γ at the point ζ_0 outside a rigid foil in the ζ plane establishes a flow described by a complex

potential $W(\zeta)$; this function can be expressed as a function $w(z)$ of $z = f^{-1}(\zeta)$. It is straightforward to show that

$$w(z) = \frac{\Gamma}{2\pi j}\log(z-d) - \frac{\Gamma}{2\pi j}\log\left[z - \left(d + \frac{R^2}{(z_0-d)^*}\right)\right] + \frac{\Gamma}{2\pi j}\log(z-z_0),$$

where $z_0 = f^{-1}(\zeta_0)$ [36]. We note that $d + \frac{R^2}{(z_0-d)^*}$ is the image of the point z_0 in the circle in the z plane.

The complex potential $W(\zeta) = w \circ f^{-1}(\zeta)$ describes the motion of any fluid point away from the vortex in the ζ plane, but not the motion of the vortex itself. The motion of the vortex is determined by the derivative of the complex potential

$$W_0(\zeta) = W(\zeta) - \frac{\Gamma}{2\pi j}\log(\zeta - \zeta_0)$$

at the point ζ_0 [36].

In the end, the equations describing the motion of z_0 will appear simpler than the equations describing the motion of ζ_0; we therefore choose to study the system in the z plane rather than the equivalent system in the ζ plane. We begin by writing

$$w(z) = w_0(z) + \frac{\Gamma}{2\pi j}\log(z-z_0),$$

so that

$$w_0(z) = W_0(\zeta) + \frac{\Gamma}{2\pi j}\log\left(\frac{\zeta-\zeta_0}{z-z_0}\right).$$

Using Taylor series to differentiate both sides of this equality with respect to z, we obtain

$$\left.\frac{dw_0}{dz}\right|_{z=z_0} = \left.\frac{dW_0}{d\zeta}\right|_{\zeta=\zeta_0} f'(z_0) + \frac{\Gamma}{4\pi j}\frac{f''(z_0)}{f'(z_0)}.$$

The chain rule requires the velocity $\dot{z}_0$ to satisfy

$$\left.\frac{dW_0}{d\zeta}\right|_{\zeta=\zeta_0} = \left(\dot{\zeta}_0\right)^* = \left(f'(z_0)\dot{z}_0\right)^* = \left(f'(z_0)\right)^*\left(\dot{z}_0\right)^*,$$

so

$$\left(\dot{z}_0\right)^* = \frac{1}{|f'(z_0)|^2}\left(\left.\frac{dw_0}{dz}\right|_{z=z_0} - \frac{\Gamma}{4\pi j}\frac{f''(z_0)}{f'(z_0)}\right).$$

In terms of the cartesian coordinates such that $z_0 = x + jy$,

$$\dot{x} = \frac{\Gamma}{2\pi}\frac{1}{|f'(z_0)|^2}\left(\frac{-(y-y_c)}{(x-x_c)^2+(y-y_c)^2} + \frac{(y-y_c)}{(x-x_c)^2+(y-y_c)^2-R^2} + k^2\,\frac{(-y^3+3x^2y-k^2y)}{(x^3-3xy^2-k^2x)^2+(-y^3+3x^2y-k^2y)^2}\right) \quad (4)$$

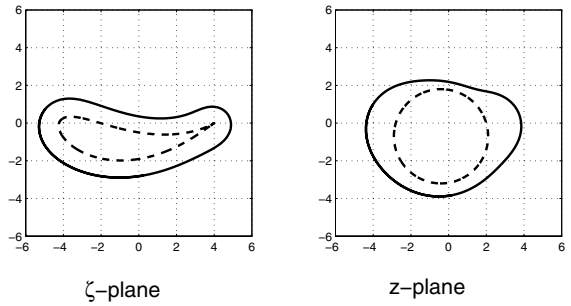

Fig. 11. Corresponding trajectories for vortex motion around a rigid foil

and

$$\dot{y} = \frac{\Gamma}{2\pi}\frac{1}{|f'(z_0)|^2}\left(\frac{(x-x_c)}{(x-x_c)^2+(y-y_c)^2} - \frac{(x-x_c)}{(x-x_c)^2+(y-y_c)^2-R^2} - k^2\,\frac{(x^3-3xy^2-k^2x)}{(x^3-3xy^2-k^2x)^2+(-y^3+3x^2y-k^2y)^2}\right), \quad (5)$$

where

$$|f'(z_0)|^2 = \frac{(x^2-y^2-k^2)^2+(2xy)^2}{(x^2+y^2)^2}.$$

Fig. 11 depicts a trajectory described around a rigid foil by a vortex in the ζ plane and the corresponding trajectory of the point z_0 in the z plane. Here $\Gamma = -5$, $x_c = -0.4$, $y_c = -0.7$, $R = 2.5$, and $k = 2$.

The preceding equations can be amended to account for deformations of the foil, circulation around the foil, and a freestream flow in the ζ plane with the addition of flows expressible in terms of complex potentials in the z plane. Deforming the foil by translating the center $d = x_c + jy_c$ of the cylinder in the z plane, for example, defines the complex potential

$$w_{\dot{d}}(z) = -\frac{R^2}{z-d}\left(\dot{x}_c + j\dot{y}_c\right);$$

the x and y components

$$\dot{x}_{\dot{d}} = \frac{R^2}{\left((x-x_c)^2+(y-y_c)^2\right)^2} \cdot\left[\left((x-x_c)^2-(y-y_c)^2\right)\dot{x}_c + 2(x-x_c)(y-y_c)\dot{y}_c\right]$$

and

$$\dot{y}_{\dot{d}} = \frac{R^2}{\left((x-x_c)^2+(y-y_c)^2\right)^2} \cdot\left[\left((y-y_c)^2-(x-x_c)^2\right)\dot{y}_c + 2(x-x_c)(y-y_c)\dot{x}_c\right]$$

of the complex velocity $(dw_d/dz)^*$ are added to the right-hand sides of (4) and (5) accordingly.

We account for changes in R with the complex potential

$$w_{\dot{R}}(z) = R\dot{R}\log(z-d),$$

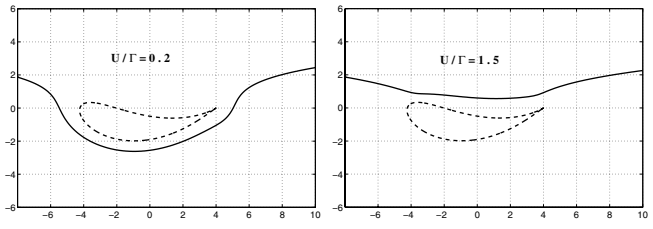

Fig. 12. Trajectories for a counterclockwise vortex around a rigid foil

for a freestream flow of speed U with the complex potential

$$w_U(z) = U\left(z - d + \frac{R^2}{z-d}\right),$$

and for a circulatory flow of strength Γ_{Kutta} with the complex potential

$$w_{\text{Kutta}}(z) = \frac{\Gamma_{\text{Kutta}}}{2\pi j}\log\left(\frac{z-d}{R}\right).$$

In order to satisfy the Kutta condition described in Section IV, we set

$$\Gamma_{\text{Kutta}} = -4\pi U y_c$$

following [35].

Combining terms, we can thus write the equations governing the motion of the vortex relative to the foil as a control-affine system with drift

$$\begin{bmatrix}\dot{x}\\ \dot{y}\\ \dot{x}_c\\ \dot{y}_c\\ \dot{R}\end{bmatrix} = \begin{bmatrix}f_1\\ f_2\\ 0\\ 0\\ 0\end{bmatrix} + \begin{bmatrix}g_{11}\\ g_{12}\\ 1\\ 0\\ 0\end{bmatrix} u_1 + \begin{bmatrix}g_{21}\\ g_{22}\\ 0\\ 1\\ 0\end{bmatrix} u_2 + \begin{bmatrix}g_{31}\\ g_{32}\\ 0\\ 0\\ 1\end{bmatrix} u_3, \quad (6)$$

where the terms f_i and g_{ij} depend on the location of the preimage (x, y) of the vortex and the position (x_c, y_c) and radius R of the cylinder in the z plane, and where the control inputs are given by $(u_1, u_2, u_3) = (\dot{x}_c, \dot{y}_c, \dot{R})$.

VI. SIMULATION OF VORTEX ENTRAINMENT

We now use the mathematical model from Section V to examine the control problem from Fig. 10. Fig. 12 depicts two possible trajectories for a clockwise vortex — like the vortex in Fig. 10 — moving around a rigid foil from left to right. A uniform flow to the right is superposed with the flow due to the vortex itself in each case; the uniform flow in the figure on the right is faster relative to the strength of the vortex than is the uniform flow in the figure on the left.

It is the natural tendency of the vortex to cross in front of the foil, away from the side on which the foil will benefit from the flow due to the vortex in the sense of Fig. 8. Only when the freestream flow is sufficiently fast will the vortex be carried past the foil on the side on which it originated.

Fig. 13 revisits the situation on the left of Fig. 12 with actuation applied in the control input u_2 from (6). Four snapshots are shown as the vortex is directed above the foil by the corresponding undulation in the foil's shape. The vortex ends up at the desired location for energy harvesting à la Fig. 9.

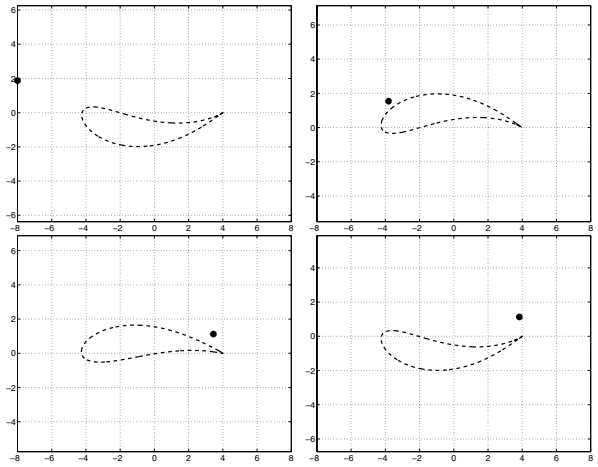

Fig. 13. Oscillation entrains the vortex to the desired side of the foil

VII. FUTURE WORK

The model developed in Section V allows us to explore the manipulation of the trajectory of the vortex through controlled deformations in the foil. It is our ultimate goal to treat this as a closed-loop control problem in which the position of the vortex at any point in time is deduced from the instantaneous flow along the surface of the foil. Schooling fish solve exactly this problem, each fish adjusting its own undulations to benefit from the wakes of its predecessors without — it would seem — direct communication among different fish. Although visual data may sometimes play a role in schooling — each fish estimating surrounding flow patterns from observations of its neighbors' movements — it has been demonstrated that even blind fish can school [37], underscoring the importance of flow sensing to cooperative fish locomotion. The estimation of a surrounding vortex flow from the pressure distribution along a hydrofoil was considered in [38]; an experimental apparatus is under development in the authors' lab which will provide distributed flow measurements along the surface of a fishlike robot using sensors mimicking the lateral lines of real fish [39].

The authors have begun to explore several other aspects of schooling locomotion, both theoretical and practical. These include the potential for direct communication to add robustness to cooperative robotic locomotion achieved through individualistic sensing, and to mediate the formation, dissolution, and reshaping of robotic vehicle schools for adaptive mobile sensing applications.

VIII. ACKNOWLEDGMENTS

The authors would like to thank Paul Newton and members of the Institute for Rational Studies for helpful discussions of vortex motion in the presence of moving boundaries; we'd also like to thank Nathan Hoople, Jonathan Craig, and Sam Jones for their contributions of data to Sections II and III.

REFERENCES

[1] M. V. Abraham and P. W. Colgan, "Risk of Predation, Hydrodynamic Efficiency, and their Influence on School Structure," *Environmental Biology of Fishes*, vol. 13, pp. 195–202, 1985.

[2] V. V. Belyayev and G. V. Zuyev, "Hydrodynamic Hypothesis of School Formation in Fishes," *Problems of Ichthyology*, vol. 9, pp. 578–584, 1969.

[3] C. M. Breder, Jr., "Vortices and Fish Schools," *Zoologica*, vol. 50, pp. 97–114, 1965.

[4] J. Herskin and J. F. Steffensen, "Energy Savings in Sea Bass Swimming in a School: Measurements of Tail Beat Frequency and Oxygen Consumption at Different Swimming Speeds," *Journal of Fish Biology*, vol. 53, pp. 366–376, 1998.

[5] R. M. Ross, T. W. H. Backman, and K. E. Limburg, "Group-Size-Mediated Metabolic Rate Reduction in American Shad," *Transactions of the American Fisheries Society*, vol. 121, pp. 385–390, 1992.

[6] B. L. Partridge and T. J. Pitcher, "Evidence Against a Hydrodynamic Function of Fish Schools," *Nature*, vol. 279, pp. 418–419, 1979.

[7] D. Weihs, "Hydromechanics of Fish Schooling," *Nature*, vol. 241, pp. 290–291, 1973.

[8] ——, "Some Hydrodynamical Aspects of Fish Schooling," in *Swimming and Flying in Nature*, T. Wu, C. Brokaw, and C. Brennen, Eds. Plenum Press, 1975, vol. II, pp. 703–718.

[9] I. Aoki, "A Simulation Study on the Schooling Mechanism in Fish," *Bulletin of the Japanese Society of Scientific Fisheries*, vol. 48, pp. 1081–1088, 1982.

[10] H. Niwa, "Self-Organizing Dynamic Model of Fish Schooling," *Journal of Theoretical Biology*, vol. 171, pp. 123–136, 1994.

[11] ——, "Newtonian Dynamical Approach to Fish Schooling," *Journal of Theoretical Biology*, vol. 181, pp. 47–63, 1996.

[12] C. W. Reynolds, "An Evolved, Vision-Based Behavioral Model of Coordinated Group Motion," in *From Animals to Animats 2: Proceedings of the Second International Conference on Simulation of Adaptive Behavior (SAB92)*, Meyer, Roitblat, and Wilson, Ed. MIT Press, 1992.

[13] P. B. S. Lissaman and C. A. Shollenberger, "Formation Flight of Birds," *Science*, vol. 168, pp. 103–105, 1970.

[14] `http://www.me.berkeley.edu/hel/calibot.htm`.

[15] K. A. Harper, M. D. Berkemeier, and S. Grace, "Modeling the Dynamics of Spring-Driven, Oscillating-Foil Propulsion," *IEEE Journal of Oceanic Engineering*, 1998.

[16] S. D. Kelly and R. M. Murray, "Modelling Efficient Pisciform Swimming for Control," *International Journal of Robust and Nonlinear Control*, vol. 10, no. 4, pp. 217–241, 2000.

[17] K. A. Morgansen, V. Duindam, R. J. Mason, J. W. Burdick, and R. M. Murray, "Nonlinear Control Methods for Planar Carangiform Fish Locomotion," in *Proceedings of the IEEE International Conference on Robotics and Automation*, 2001.

[18] M. Nakashima, K. Kaminaga, and K. Ono, "Experimental Study of Two-Joint Dolphin Robot," in *Proceedings of the 1st Annual Symposium on Aqua Bio-Mechanisms*, 2000.

[19] S. Saimek and P. Li, "Motion Planning and Control of a Swimming Machine," 2003, Submitted to the *International Journal of Robotics Research*.

[20] M. S. Triantafyllou and G. S. Triantafyllou, "An Efficient Swimming Machine," *Scientific American*, vol. 272, pp. 64–70, 1995.

[21] S. J. Lighthill, *Mathematical Biofluiddynamics*. SIAM, 1975.

[22] T. Y. Wu and C. J. Brokaw and C. Brennen, editors, *Swimming and Flying in Nature, volumes I and II*. Plenum, 1975.

[23] T. B. Curtin, J. G. Bellingham, J. Catipovic, and D. Webb, "Autonomous Oceanographic Sampling Networks," *Oceanography*, vol. 6, pp. 86–94, 1989.

[24] P. Bhatta and N. E. Leonard, "Stabilization and Coordination of Underwater Vehicles," *Proceedings of the IEEE Conference on Decision and Control*, 2002.

[25] P. Ogren, E. Fiorelli, and N. E. Leonard, "Formations with a Mission: Stable Coordination of Vehicle Group Maneuvers," in *Proceedings of the Fifteenth International Symposium on the Mathematical Theory of Networks and Systems*, 2002.

[26] E. Kanso, J. E. Marsden, C. W. Rowley, and J. Melli-Huber, "Locomotion of Articulated Bodies in a Perfect Fluid," submitted to *Journal of Nonlinear Science*, 2004.

[27] S. D. Kelly, "The Mechanics and Control of Driftless Swimming," To appear, *SIAM Journal on Control and Optimization*.

[28] L. M. Milne-Thomson, *Theoretical Aeroodynamics*. Dover, 1973.

[29] S. D. Kelly, H. Xiong, and R. B. Hukkeri, "Mechanics, Dynamics, and Control of a Single-Input Aquatic Vehicle With Variable Coefficient of Lift," Submitted to *IEEE Transactions on Robotics*, 2004.

[30] R. J. Mason, "Fluid Locomotion and Trajectory Planning for Shape-Changing Robots," Ph.D. dissertation, California Institute of Technology, 2002.

[31] L. Föppl, "Wirbelbewegung hinter einem Kreiszylinder," *Sitz. K. Bäyr Akad. Wiss*, vol. 1, pp. 7–18, 1913.

[32] D. Hill, "Vortex Dynamics in Wake Models," Ph.D. dissertation, California Institute of Technology, 1998.

[33] B. N. Shashikanth, J. E. Marsden, J. W. Burdick, and S. D. Kelly, "The Hamiltonian Structure of a 2-D Rigid Circular Cylinder Interacting Dynamically with N Point Vortices," *Physics of Fluids*, vol. 14, pp. 1214–1227, 2002.

[34] A. V. Borisov, "Motion of a Circular Cylinder and n Point Vortices in a Perfect Fluid," *Regular and Chaotic Dynamics*, vol. 8, no. 4, pp. 449–462, 2003.

[35] L. M. Milne-Thomson, *Theoretical Hydrodynamics*. Dover, 1996.

[36] P. K. Newton, *The N-Vortex Problem*. Springer-Verlag, 2001.

[37] T. J. Pitcher, B. L. Partridge, and C. S. Wardle, "Blind Fish Can School," *Science*, vol. 194, p. 964, 1976.

[38] P. Li and S. Saimek, "Modeling and Estimation of Hydrodynamic Potentials," in *Proceedings of the IEEE Conference on Decision and Control*, 1999, pp. 3253–3258.

[39] Z. Fan, J. Chen, J. Zou, D. Bullen, C. Liu, and F. Delcomyn, "Design and Fabrication of Artificial Lateral Line Flow Sensors," *Journal of Micromechanics and Microengineering*, vol. 12, pp. 655–661, 2002.